IEEE Access
Multidisciplinary ⋮ Rapid Review ⋮ Open Access Journal

Received 4 March 2025, accepted 17 March 2025, date of publication 1 April 2025, date of current version 11 April 2025.

Digital Object Identifier 10.1109/ACCESS.2025.3556920

RESEARCH ARTICLE

Offline Versus Real-Time Grasp Prediction Employing a Wearable High-Density Lightmyography Armband: On the Control of Prosthetic Hands

BONNIE GUAN [1], (Student Member, IEEE), RICARDO V. GODOY [1], (Student Member, IEEE), MOJTABA SHAHMOHAMMADI [1], ANANY DWIVEDI [2], AND MINAS LIAROKAPIS [1], (Senior Member, IEEE)

[1]New Dexterity Research Group, Department of Mechanical and Mechatronics Engineering, The University of Auckland, Auckland 1010, New Zealand
[2]Artificial Intelligence (AI) Institute, Division of Health, Engineering, Computing, and Science, University of Waikato, Hamilton 3216, New Zealand

Corresponding author: Bonnie Guan (bgua324@aucklanduni.ac.nz)

This work involved human subjects or animals in its research. Approval of all ethical and experimental procedures and protocols was granted by the University of Auckland Human Participants Ethics Committee (UAHPEC) under Application No. #26227.

ABSTRACT Several studies over the last decades have investigated the use of myoelectric upper-arm prostheses to restore lost functionality and perform complex activities of daily life. Muscle-machine interfacing methods employing electromyography, sonomyography, forcemyography, and mechanomyography, have been developed offering users intuitive control of prostheses. However, these methods suffer their own drawbacks and the practical, robust, real-time control of prostheses in the execution of complex everyday life tasks remains difficult to accomplish. In this study, a wearable high-density lightmyography armband is proposed, and the offline and real-time grasp prediction schemes are compared in an attempt to deepen our understanding in real-time decoding employing lightmyography signals. Thus bringing lightmyography closer to advanced real-time prosthetic control scenarios. Offline experiments were conducted where models decoding 10 classes were trained and tested, achieving accuracies exceeding 91% with a mean of 94.11% when a Random Forest model was employed and a mean of 95.87% when a Convolutional Neural Networks model was employed. However, as models were deployed in real-time, a decline in performance was notable, reducing the accuracies to 60-70%. Other limitations were observed in this transition. Although average accuracies were high, the precision and recall for a small fraction of grasps were often low, hindering overall real-time performance. Moreover, prolonged usage led to decreased decoding accuracy, with accuracies dropping to below 35%, indicating that fatigue, sweat, or sensor shift may have affected the signals over time. Thus for the real-time application of lightmyography, it is recommended to discriminate between a smaller number of classes for which accuracies are higher (around 80% for 6 classes without prolonged use).

INDEX TERMS Human–machine interfaces, muscle-machine interfaces, grasp classification, real-time decoding, prosthetic control.

I. INTRODUCTION

Upper arm amputees experience negative changes in their quality of life, with the hand being the most important tool that we, as humans, use to interact with our surroundings [1], [2]. Thus, prosthetic devices allow amputees to regain their lost dexterity, and they provide them the opportunity to engage with the environment confidently [3]. Studies evaluating prosthesis use have suggested that prosthetic hands can increase proficiency in conducting activities of daily

The associate editor coordinating the review of this manuscript and approving it for publication was Alberto Botter .

living (ADL) [4], can increase chances of employment [5], and can have positive effects on social confidence [6]. As prosthetic technology becomes more advanced in conjunction with rapid developments in robotics, prosthetic hands are becoming increasingly capable, with sophisticated sensing and multiple degrees of freedom (DoF). It is then critical that users are able to smoothly control their devices with ease.

The most common method of implementing a human-machine interface (HMI) for prosthetic devices involves using surface electromyography (sEMG). The control signals are obtained directly from the muscles, and thus the hands of the user are not required, allowing for intuitive control [7], [8], [9]. As a result, electromyography (EMG) has seen applications in the fields of bionics, robotics, rehabilitation, and health monitoring [10]. Wearable systems are particularly practical in the field of bionics and have seen success in the control of exoskeletons [11] and prosthetics [12], [13].

However, in general, although cheaper versions exist, using EMG-based interfaces becomes expensive, especially as you add more sensors. The signals are of very small magnitudes, and typically, EMG interfaces require sophisticated electronics, contributing to the high cost of commercially available EMG-based prosthetics [14]. EMG signals are also prone to electromagnetic interference from the environment, as well as muscle cross-talk, making readings extremely noisy and difficult to decode robustly. Additionally, patterns produced in the EMG signals can be affected over time due to sweat, electrode shifting, and fatigue of the user [15]. Amputees using myoelectric prostheses often give them up due to their weight and limited functionality [16].

Other methods of muscle-machine interfacing (MuMI-ing) have been studied beyond EMG, such as sonomyography (SMG) [17], [18]. SMG relies on interpreting the muscle changes in ultrasound images of the arm's cross-section. Compared to EMG, SMG directly extracts morphological changes of the muscles, tracking muscle thickness, length, and shape, reducing susceptibility to noise. However, SMG relies on expensive equipment for ultrasonography, and often the setup is bulky, making it impractical to implement for prosthetic control [19]. Cheaper MuMIs have also seen some interest. Studies have implemented forcemyography (FMG), which relies on pressure or force sensors placed on the surface of the skin to detect changes in the muscle shape as they contract. These signals can then be decoded using machine learning methods to determine human intention [20], [21], yielding similar decoding results in grasp decoding and force regression compared to using EMG signals. Many FMG wearables have been proposed in research that reach under \$200 USD in production cost [20], [22]. Mechanomyography (MMG), which detects the mechanical vibrations on the skin, typically with piezoelectric sensors or condenser microphones, as the user contracts the muscles, has also been proposed to control prosthetic hands [23], [24]. These methods rely on mechanical changes in the arm

TABLE 1. Comparison of the properties between the previous LMG modules and the proposed HDLMG module. Although the new module is slightly larger, and has a lower sampling rate, the number of sensors and resolution is much greater. About 95% of the cost is from the FPC, which is outsourced.

Characteristic	Old LMG Module 	New HDLMG Module 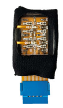
Size	14 x 38 x 30 mm	10 x 62 x 27 mm
No. of Sensors	1	8
Resolution	10-bit	12-bit
Sampling Rate	55 Hz (for 5 modules)	50 Hz (for 5 modules)
Material	Rigid PCB	Flexible PCB
Cost Estimate	30 USD (for 1 Module)	80 USD (for 1 module)

rather than physiological changes, and are popular options for wearable interfaces [25] due to the accessibility of the sensors. Currently, only EMG armbands are commercially available, with the most popular being the discontinued Thalmic Labs MyoArmband priced at \$200 USD. Oxymotion has also released the gForce-Pro, with higher capabilities compared to the MyoArmband, but priced at \$1250.

In our previous work, a new muscle machine interfacing method was proposed called lightmyography (LMG) [26], [27]. LMG uses the transmission of light through a silicon medium onto the skin, measuring the changed in intensity of light. Light is partially absorbed and reflected on the skin surface and within the layers of the skin. LMG uses differing wavelengths of light, penetrating the skin at different depths [28]. In doing so, the change in blood flow through that area can be detected following the principles of photoplethysmography [29]. This proposed interfacing method was compared with EMG-based gesture classification, with comparable offline decoding results averaging above 95% when five gestures are decoded. Please note that LMG only relies on simple circuitry (similarly to FMG and LMG), can be produced very affordably, and is more robust to electromagnetic interference.

Given that LMG is comparable to EMG in the offline sense, this study aims to bring LMG closer to real-life prosthetic control by further improving the technology, and analyzing real-time decoding results, studying more closely the real-time behavior of LMG deocding. In doing so, we reveal the issues that need to be taken into consideration for the design of LMG prosthetic systems. Many studies that examine decoding of MuMIs report offline results, such as the studies that employ the NinaPro dataset [30]. Although there are studies examining real-time implementations, especially with EMG [31], [32], [33], [34], these studies are still few in comparison. It is important to understand the challenges in real-time implementation to design suitable prosthetic control systems, particularly with a novel method of interfacing such as LMG. In this paper, a direct improvement was made to

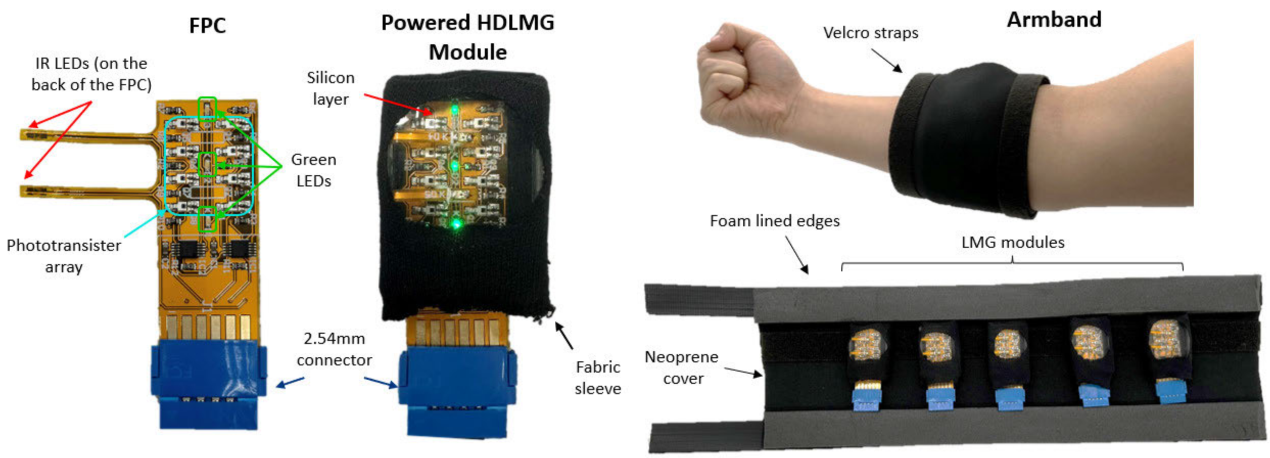

FIGURE 1. HDLMG FPC that includes 8 phototransistors in an array, along with 3 green LEDs and two IR LEDs. A small fabric sleeve holds the FPC onto a silicon layer. The fabric sleeves attach themselves to a neoprene cover, which blocks out a majority of the light. The edges are lined with foam so that the band conforms around the user's arm, preventing light from entering the sides.

the LMG armband from [26], proposing a new version of the LMG technology. We call this new version high density LMG (HDLMG), inspired by high density EMG (HDEMG) methods of prosthetic control [35], [36], [37], which has been used to make HDEMG armbands [38].

With the new armband, a series of experiments were conducted to examine the offline and online capabilities of models trained with HDLMG signals, bringing LMG technology closer to practical use. Offline experiments were first conducted with multiple participants, and models were trained with classical machine learning and deep learning methods. Two participants then moved forward with online, real-time experiments. Two experiments were conducted: Multi-session experiments in which the armband was removed before new data was collected to train a model to be deployed for decoding 3, 6, and 10 classes, and single-session experiments in which data was collected a single time and segmented to train models decoding 3 to 10 classes. During this investigation, the limitations in moving from offline experiments to online deployment are revealed and discussed along with LMG design considerations for future research.

II. DESIGN

A. LIGHTMYOGRAPHY MODULES

Table 1 shows a comparison between the LMG module proposed previously in [26] and the new HDLMG module. The HDLMG modules are slightly larger by 780 mm^3, have a sampling rate that is 5 Hz lower, and because the PCBs are no longer manufactured in house, the cost is much higher, although, with higher production rates, the cost per module is expected to decrease. However, there are now 7 more photosensors on each module, and the resolution is now 12-bit as opposed to 10-bit, overall a direct upgrade.

Each HDLMG module consists of an FPC with 8 phototransistors laid out in a 2 x 4 array, 3 Green light emitting diodes (LEDs), and two IR LEDs. The layout of the components can be seen in Fig. 1, and was designed based on the size of the previous version. The IR LEDs are placed on the back of the FPC, so that they fold over a silicon layer, ensuring they are 5 mm away from the rest of the board. This means the IR LEDs will be touching the skin when the modules are placed on the forearm, while the green LEDs will be 5 mm away, following the experiments and design conducted in [26]. By using an FPC rather than a traditional rigid printed circuit board, the modules should, in theory, wrap around the user's arms, allowing for more uniform contact over the entire surface of the modules. The sensor data is input into two ADS1015 ADCs set to two different I2C addresses, then a standard 2.54 mm connector allows the FPC to be connected to an Arduino or other microcontroller, which can read the sensor data through the I2C communication, as well as control the LEDs and power the module. To read multiple modules, a TCA9548A I2C multiplexer is used. Fig. 2 shows the interaction between the components on the FPC, as well as how the HDLMG module connects to the computer for data recording and processing. The FPC is fixed to a silicon layer using a thin fabric sleeve that can attach the modules onto a neoprene armband.

B. LIGHTMYOGRAPHY ARMBAND

The armband is shown in Fig. 1. The main band is made from neoprene with velcro lined on the inside. The modules can be attached to the velcro on the band depending on the user's forearm size. A foam lining inside the edges of the band conforms to the skin to block out light seeping into the sides. 5 modules are used in the experiments in this paper based on the same number of modules used in our previous work, and while more can be added based on the size of the user's forearms, the sampling rate of the sensors would decrease. Consequently, if a higher sampling rate is desired, fewer modules can be used. Similarly to the previous design, the green and IR LEDs blink alternately at intervals of 250 ms. The ability of the armband to block out environmental light was tested. A white LED was oscillated

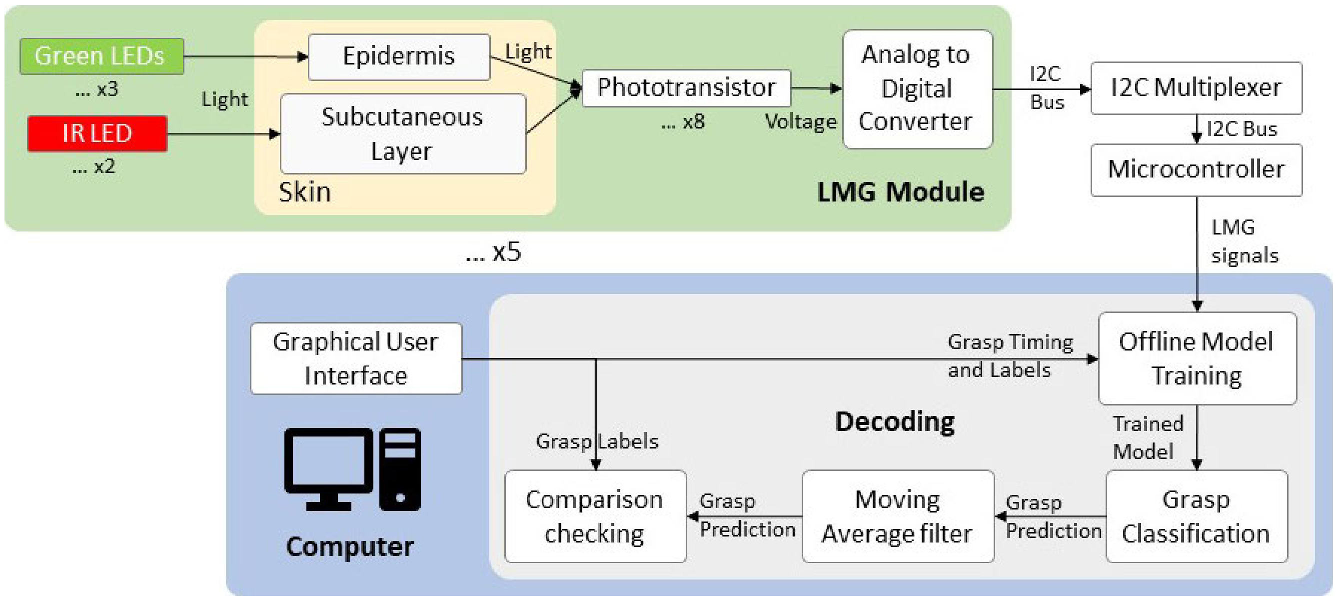

FIGURE 2. A flowchart showing how the components of the FPC interact with each other, and how the FPC communicates with a computer which can process the HDLMG readings.

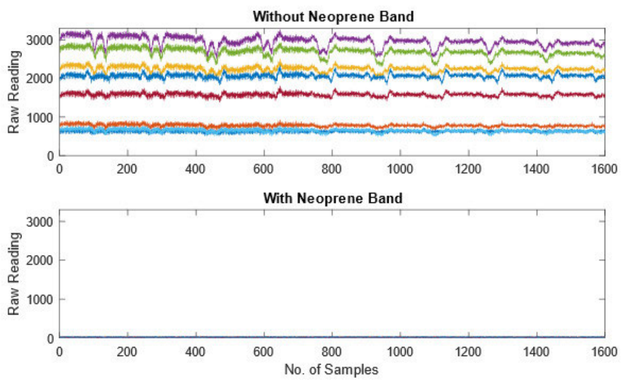

FIGURE 3. A sample plot of data recorded as the white LED oscillates above the modules (8 sensors per module). With the armband covering the modules, ambient light is blocked out, with the highest values recorded being 32. Changes in the light oscillations are also minimized. The average RMSD of the signals relative to their means was 41.76±9.26 without the band and 3.38±0.057 with the cover.

above two modules - one inside the armband and one held onto the arm with just a strap. 10 oscillations were recorded 3 times in the direction parallel to the arm, and another 3 sets of 10 oscillations were recorded moving perpendicular to the arm. The participant kept their arm still during this experiment. A plot of one of the trials is shown in Fig. 3. Without the armband cover, ambient light can be seen clearly on the plots, while the largest reading from the module inside the cover which was 32. Patterns that arise from the LED light are also minimized. The resulting signals were smoothed with a moving average window of 5 samples, then the root mean squared deviation (RMSD) of the signals with respect to their means was calculated. The average RMSD of the recorded data from the module inside the armband was 3.38 with a standard deviation of 0.057, while the average RMSD of the data recorded outside the armband was 41.76 with a standard deviation of 9.26 indicating that the light changes were well obstructed.

III. METHODS

A. DATA PREPROCESSING

In order to prepare the data to be fed to the machine learning classification model, the LMG data goes through data preprocessing steps. It is worth mentioning that, in contrast to EMG, the LMG signals do not require filtering and feature extraction steps. Normalization of the LMG signals is not required during preprocessing steps, as batch normalization layers are incorporated within the deep learning architecture, increasing training speed and eliminating the need for normalization during preprocessing steps [40]. Batch normalization performs the normalization for each mini-batch, and backpropagates the gradients through the normalization parameters. We employed a sliding window of 200 ms with a stride of 20 ms to extract samples from the LMG data collected. The sliding window was chosen to be larger than 125 ms to avoid high biases and variance [41] and smaller than 300 ms due to real-time constraints of prosthetic control systems [42]. The data was balanced to guarantee that we have the same number of samples for each of the ten classes to avoid bias toward a particular class. To do so, we randomly downsampled the majority classes until each class presented the same number of instances.

B. CLASSIFICATION MODEL

For hand grasp decoding, we employed two well-established machine learning techniques for classifying the LMG signals. The first technique employed was a Random Forest (RF)

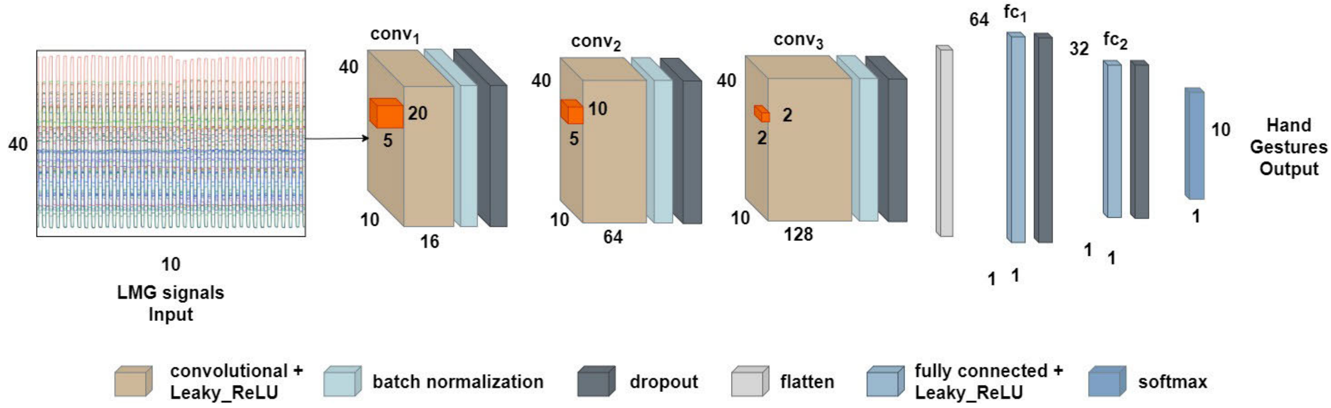

FIGURE 4. CNN model employed for decoding LMG data. Three convolutional blocks composed of convolutional, batch normalization, and dropout layers are followed by fully connected and dropout layers. The convolutional filters are shown in orange. A dropout rate of 0.2 was employed. A final softmax layer with ten neurons performs the grasp classification.

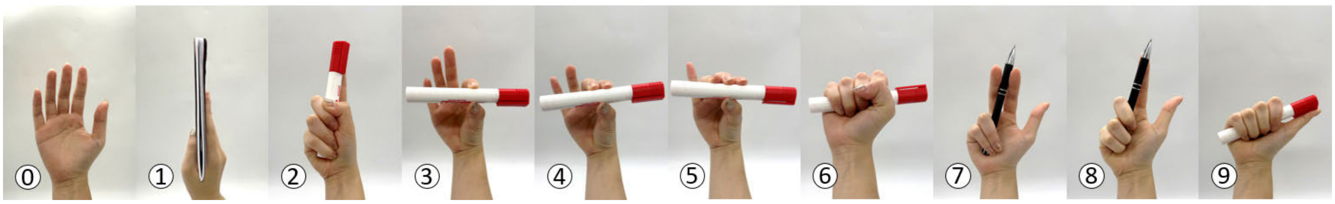

FIGURE 5. The 9 grasps (and rest) that were mapped to the robotic hand that were selected for classification. With these grasps, most of the taxonomy proposed by [39] could be replicated.

classifier [43]. RF is an ensemble learning method for classification and regression that works by constructing multiple decision trees at training time. In classification tasks, the output of RF is determined by the majority vote among the trees, which enhances accuracy by averaging across several deep decision trees and reducing overfitting risks. The proposed RF comprised 100 trees. The second technique was a Convolutional Neural Network (CNN) as shown in Fig. 4. CNNs are employed in several applications due to their ability to extract spatial characteristics and identify patterns of a given input data. The CNN used in this paper comprises three convolutional blocks, two fully connected layers, and a final softmax layer to predict the hand grasps. Each convolutional block comprises convolutional, batch normalization, leaky ReLU activation function, and dropout [44] layers. These two techniques were chosen based on our previous works [26] and on the fact that they can present good predictive performance and do not require much time to train as deeper DL techniques, which is paramount during the development of prosthetic frameworks.

C. TRAINING AND EVALUATION

The machine learning models were developed in Python using TensorFlow and Keras. The models were trained and validated using the 10-fold cross-validation method, leaving one repetition out for testing per fold. Therefore, 90% of the dataset was used for training and 10% for validation. During the training of each CNN model, the loss function was the sparse categorical cross-entropy. Optimization was performed using Adam [45]. The decoding efficiency of the models was assessed using accuracy. The experiments were performed on the New Zealand eScience Infrastructure (NeSI) high-performance computing facilities that are equipped with appropriate GPUs.

IV. EXPERIMENTS

A. DATA COLLECTION

The University of Auckland Human Participants Ethics Committee (UAHPEC) approved the study with the accepted protocol with reference number #26227. All experiments were performed in accordance with relevant guidelines and regulations. Prior to the study, the user of the system provided written and informed consent to the experimental procedure. 10 individuals participated in this study (ages 20 to 35). More information about each subject can be found in Table 2. Each participant was asked to wear the LMG armband on their forearm and then to perform 10 seconds of rest in which the arm was completely relaxed, followed by 10 seconds of a grasp. A similar method of data collection has been used multiple times by the authors, including for cases with EMG control [26], [46], [47], [48]. This repeated 9 more times while the LMG signals were recorded, giving each recording 10 repetitions. Visual cues on a computer screen were given to count down each transition between rests and grasps, whilst also labeling the data collected. LMG data was collected at a rate of 50 Hz while the participants performed this sequence.

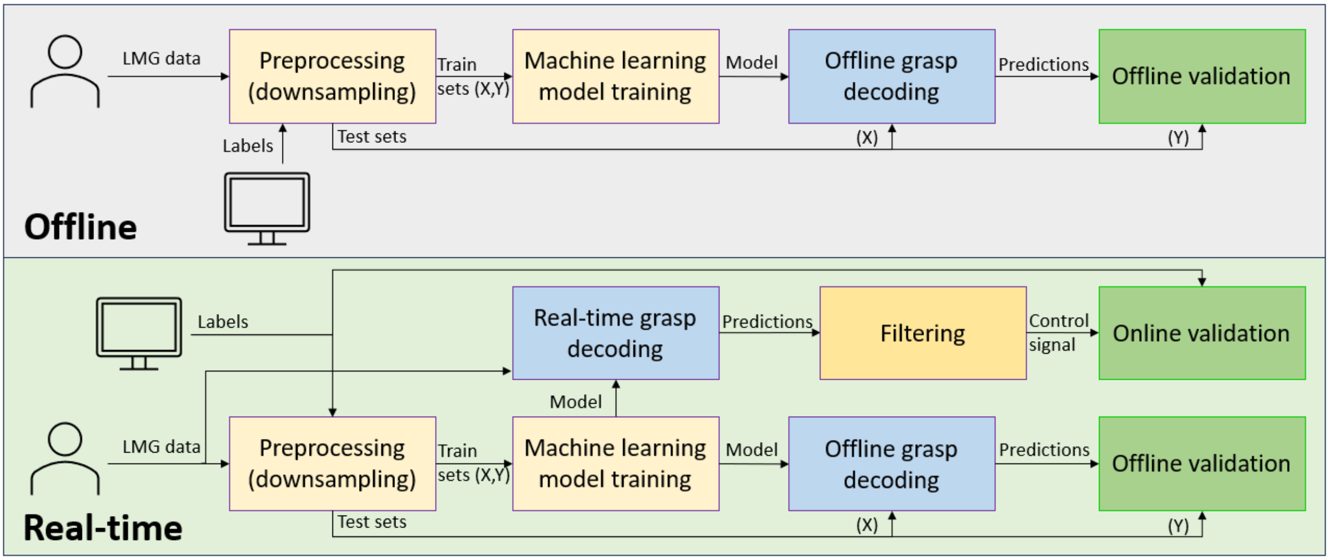

FIGURE 6. A flowchart showing the data flow in the offline model training and real-time experiments.

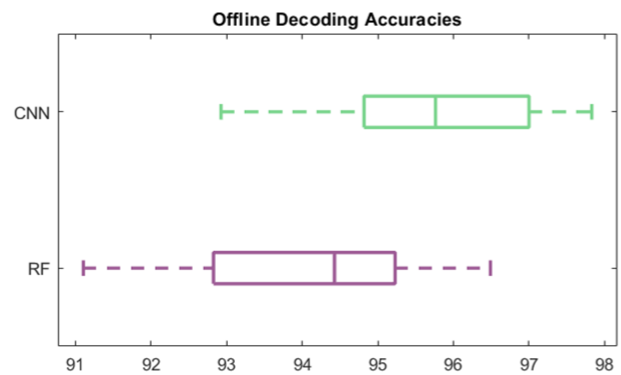

FIGURE 7. Boxplots comparing the offline decoding using RF and CNN. There is significant difference between the two models (p=0.1.416e-06) although the difference in the means is small (<2%).

9 grasps derived in our previous work [49] were recorded in this manner, which can be seen in Fig. 5 (10 classes including the rest state). If participants began to feel fatigued during the duration of the data collection, they were allowed to move and stretch their arm, so long as the LMG armband did not move excessively.

B. REAL-TIME GRASP PREDICTION

Two subjects (male, right-handed, 26 years old and female, right-handed, 24 years old) participated in the real-time decoding experiments. They were first asked to follow a similar procedure described in Section IV-A. However, instead of performing the same grasps 10 times per recording, the user was asked to perform each of the different grasps once per recorded repetition. Therefore, the participant would begin with their arm and hand at rest for 10 seconds, then perform grasp 1 (shown in Fig 5) for 10 seconds, followed by rest again, then grasp 2 for another 10 seconds. This comprised one repetition with 3 classes (2 grasps + rest). A total of 5 repetitions were collected. The data was then used to train a machine learning model, using the 4th repetition as test data.

TABLE 2. Subjects' information. *M* stands for male, *F* for female, and *Hand.* for handedness.

Subject	1	2	3	4	5	6	7	8	9	10
Sex	M	M	M	M	F	M	F	M	F	F
Hand.	Right	Right	Right	Right	Right	Right	Right	Left	Right	Left

Live HDLMG data would then be streamed into the model, and the participant would perform the repetition another 2 times. This time, the model output was fed through a smoothing filter of window size 10, then the final gesture was recorded alongside the HDLMG data and the true grasp labels so that the online accuracy could be determined.

This procedure would be repeated for 6 classes, and 10 classes. However, when repeating the procedure, the user would take the armband off, take a break, and then put it back on, separating the experiment session. These experiments were termed **multi-session** real-time experiments. As we move from offline analysis, where decoding accuracies are high, we expect to see a drop in the accuracy, thus we begin with a lower number of classes for researchers to use as a guide for the design of future real-time LMG systems.

Additionally, on seeing the results of the multi-session experiments, the same participants were asked to return for a further exploration. The order of the grasps was rearranged based on the RF confusion matrix seen in Fig. 8 so that grasps that were easier to decode were performed first. The grasps were also arranged afterward to prevent similar grasps from being executed one after the other, to prevent poor decoding with a low number of grasps. The new order of the grasps, based on the labels in Fig 5, was 5, 9, 7, 2, 4, 8, 3, 6, 1. Data

TABLE 3. Offline decoding accuracies, in percentage, achieved by the two machine-learning classification models. *AVG* stands for average and *SD* for standard deviation. The greater accuracy for each subject is highlighted in green.

Fold	Subject									
	1	**2**	**3**	**4**	**5**	**6**	**7**	**8**	**9**	**10**
RF										
0	95.34	92.92	87.8	82.88	87.4	89.9	89.98	93.99	90.81	87.25
1	97.69	89.86	95.06	95.59	85.79	94.52	97.12	93.29	93.57	92.54
2	97.7	96.48	94.66	97.72	93.34	95.14	97.22	94.27	93.49	94.83
3	96.77	95.23	97.38	96.71	93.71	94.48	96.9	97.02	93.76	96.29
4	96.28	95.46	96.81	97.18	93.26	94.23	97.33	92.94	92.58	96.53
5	97.36	95.54	97.08	97.44	91.79	94.13	97.65	95.58	93.89	94.4
6	96.66	96.27	96.69	97.69	92.92	94.79	96.43	96.59	92.98	96.28
7	96.37	94.9	96.94	96.98	92.8	94.11	98.51	97.52	93.13	85.28
8	96.94	95.87	95.97	97.32	92.8	94.47	98.06	96.51	93.59	95.12
9	93.82	89.26	88.36	92.75	87.28	82.51	91.58	93.88	84.44	92.76
AVG	**96.49**	**94.18**	**94.68**	**95.23**	**91.11**	**92.83**	**96.08**	**95.16**	**92.22**	**93.13**
SD	**1.18**	**2.63**	**3.59**	**4.59**	**3.03**	**3.91**	**2.88**	**1.68**	**2.88**	**3.90**
CNN										
0	97.33	95.62	96.43	92.79	92.1	93.56	97.81	95.13	94.01	94.98
1	97.89	95.46	91.18	97.89	90.22	95.01	98.18	95.98	93.78	95.24
2	97.25	97.23	96.24	98.11	94.89	95.76	97.92	97.01	94.18	96.12
3	98.09	96.2	97.89	97.27	94.23	96.23	97.67	96.78	94.07	96.87
4	98.01	96.11	97.33	97.85	93.84	96.22	97.75	95.72	92.82	96.17
5	97.85	96.98	98.21	97.93	92.89	94.96	98.28	97.19	95.23	96.02
6	97.56	96.23	97.14	98.13	94.39	95.64	96.79	97.99	94.22	97.11
7	96.45	94.89	98.03	98.25	92.99	96.32	98.76	97.19	92.39	93.25
8	97.83	95.38	96.34	97.99	94.01	96.42	97.99	97.93	94.13	96.03
9	95.24	91.99	90.38	93.74	89.72	88.12	97.12	95.12	88.33	93.02
AVG	**97.35**	**95.61**	**95.92**	**97.00**	**92.93**	**94.82**	**97.83**	**96.60**	**93.32**	**95.48**
SD	**0.89**	**1.46**	**2.80**	**2.00**	**1.76**	**2.51**	**0.56**	**1.06**	**1.92**	**1.39**

was collected in a single session for all 9 grasps, and separate models were trained for 3, 4, 5 all the way to 10 classes. In the same session without taking off the armband, participants would then test each of the classification models, perform a repetition 2 times for each of the 8 models, while the output of the model with filtering was recorded. These experiments were termed **single-session** real-time experiments. The LMG data pipeline of both the offline and real-time experiments is shown in Fig. 6.

V. RESULTS AND DISCUSSION

A. OFFLINE DECODING RESULTS

A summary of the grasp classification accuracies achieved by the decoding models are presented in Fig. 7, while the details of each testing fold are revealed in Table 3. It can be seen that the CNN model presets a better decoding accuracy and standard deviation for all the subjects than the RF model, achieving average accuracies as high as 97.83% for decoding 10 classes. Both models achieve average accuracies higher than 91% for all the subjects. The confusion matrix for the CNN and RF of one subject is shown in Fig. 8.

On average, the CNN performed better than the RF, statistical analysis using the paired-sample t-test shows significant difference between the two models (p= 1.416e-06). However, the difference in the means is small (< 2%), and

TABLE 4. Online decoding accuracies achieved from the **multi-session** experiments. The participants took breaks between each session, and data was recollected for each model trained on differing numbers of grasps. This is compared to the accuracy when the same model was tested offline. The accuracies are presented in percentage, *acc* stands for accuracy, and *rep* for repetition.

Subject	No. of decoded classes	Offline acc as tested on 4th rep	Average online acc
1	3	98.09	98.07
	6	90.43	79.72
	10	84.25	70.96
2	3	82.38	92.95
	6	70.01	79.5
	10	66.01	61.77

TABLE 5. Online decoding precision, recall, and F1 score achieved from the multi-session experiments. All values are reported as percentages. Lower performing classes are highlighted in red (<60%) while mid performing classes are highlighted in orange (60% to 80%).

	Subject 1									Subject 2								
	Precision			Recall			F1 Score			Precision			Recall			F1 Score		
	No. of decoded classes									No. of decoded classes								
	3	6	10	3	6	10	3	6	10	3	6	10	3	6	10	3	6	10
0	94.7	70.5	66.9	100	94.96	100	97.25	79.83	80.14	90.45	77.1	74.6	87.59	100	99.39	88.87	86.32	84.8
1	100	85.55	100	100	99.75	54.56	100	91.43	70.29	89.05	100	67.7	92.38	65.69	54.8	90.54	76.48	59.67
2	100	100	81.45	94.23	100	52.82	96.99	100	64.03	100	100	37.45	98.89	100	53.27	99.44	100	43.69
3		73.35	83		79.93	68.59		76.21	74.82		100	99.4		60.2	72.97		73.61	83.97
4		63.1	50		45.57	16.22		50.54	24.49		74.25	46.6		51.11	86.33		59.97	60.51
5		88.8	55.3		58.11	98.53		62.95	70.77		59.55	70		100	24.88		74.64	35.65
6			52.65			85.41			64.63			16.15			14.41			15.23
7			78.7			98.4			86.42			48.7			34.77			40.54
8			100			65.52			74.84			99			90.54			94.5
9			82			69.58			70.18			97.45			86.33			91.15

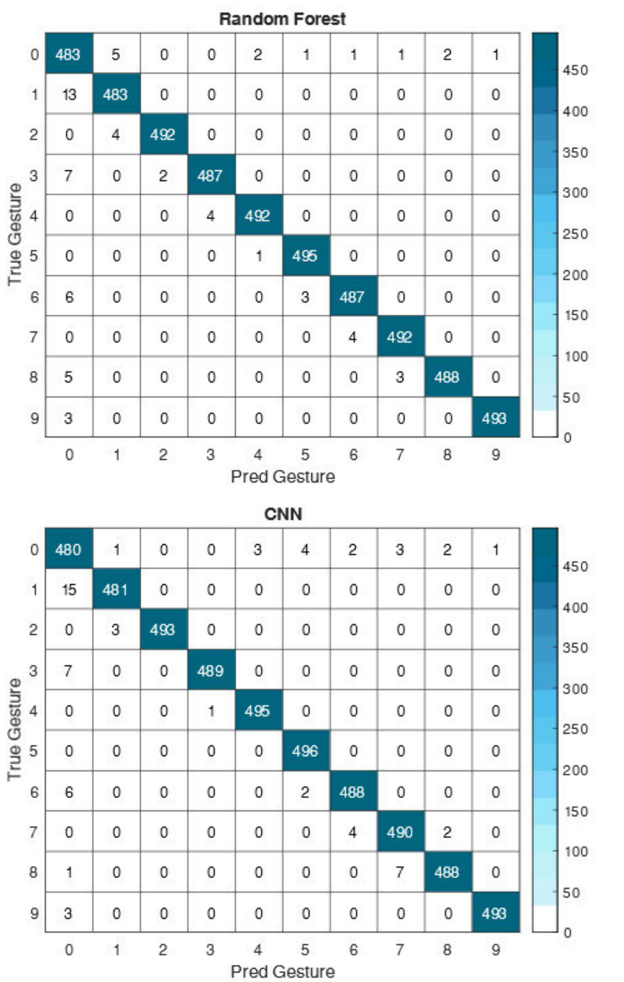

FIGURE 8. Confusion matrices showing the decoding accuracy for each of the ten classes achieved by RF and CNN models for a given participant's testing fold.

the overall good performance of the RF models indicates that LMG signals can be decoded even by classic and less robust machine learning techniques. Classical machine learning methods require less computational resources to train and deploy, and yet present high decoding performance, as can be observed in EMG studies [48]. Thus enhancing the applicability of the LMG-based HMI for scenarios where powerful GPUs are not available for training and/or deployment which may be the case for cheaper embedded systems. The prediction time of both models to process and predict one sample was measured. It was found that RF takes an average of 0.0517 ms, while CNN takes 0.2657 ms to predict one sample of data. Therefore, given that both models presented similar decoding accuracies, the RF model was chosen for the real-time experiments, given that its prediction time was more suitable for real-time applications. One idea for further consideration is the use of more advanced deep learning techniques. However, as large quantities of data cannot be collected without the time cost being impractical for a prosthetic application, it would not be suitable to select a deep learning model, especially considering the computational costs, which will add to the cost of the overall system.

B. REAL-TIME DECODING RESULTS

The real-time decoding accuracies of the multi-session experiments are shown in Table 4 while the precision, recall, and F1 score of each class are shown in Table 5. RF models were chosen for their faster prediction times while also being more suitable for embedded systems with low computational power. Accuracies are calculated by trimming 1 second of data from both ends of a repetition to remove transitional states, and then calculating the percentage of predictions that matched the grasp being performed. The offline accuracies of the models, as tested on the 4th repetition of offline data, are also presented. As expected, the models trained for a lower number of classes (grasps) achieve higher decoding accuracy. As the model is deployed online, the accuracy also sees large changes, with some models performing better online, while, for the most part, accuracy drops. The largest drop being from 84.25% to 70.96% when comparing the results achieved offline and online. No statistical differences were observed with the paired-sample t-test in all 3 ($p=0.2994$), 6 ($p=0.9619$), or 10 ($p=0.3034$) decoded gestures between the offline and online decoding, however, we must keep in mind that the sample size is 2 and any statistical analysis is likely not meaningful. Subject 1's confusion matrix is also shown in Fig. 9.

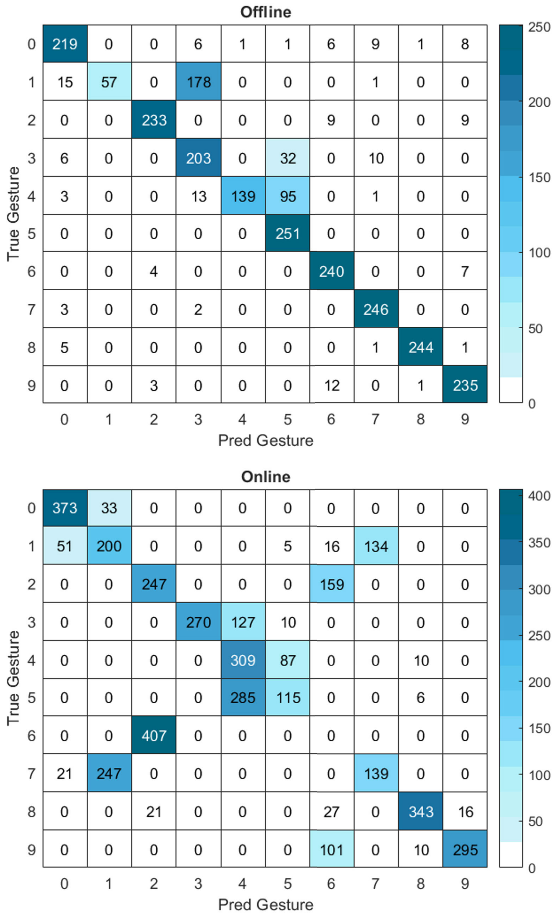

FIGURE 9. Subject 1's confusion matrices showing the decoding accuracy for each of the ten classes achieved by when tested offline, and deployed by same model in real-time.

Seeing such drastic differences in the model's real-time performance for each number of grasps, the single-session experiments were conducted in which the placement of the HDLMG armband stayed the same. Table 6 shows the results of the single-session experiments. This time, results are more consistent, showing a gradual decrease in accuracy as more grasps are introduced. However, decoding accuracy has dropped towards the higher number of grasps, with subject 2 going as low as 18.99%. Despite large differences, paired-sample t-testing revealed no significant difference with any number of classes: 3 ($p=0.2732$), 4 ($p=0.0572$), 5 ($p=0.1523$), 6 ($p=0.1756$), 7 ($p= 0.0712$), 8 ($p=0.1787$), 9 ($p=0.128$) and 10 ($p=0.1087$) at a null hypothesis $p>0.05$. However, statistical testing at a low number of samples leads to large confidence intervals, so we cannot reliably infer anything from the results of the statistical testing. The goal of future research will be to involve more subjects in order to produce more conclusive results.

C. LIMITATIONS TRANSITIONING FROM OFFLINE TO REAL-TIME AND LMG DESIGN CONSIDERATIONS

Although offline decoding results reached high decoding accuracies of 91%+ (as can be seen in Table 3), it is apparent that in an online, real-time setting, this is not the case. Only a small sample size of two participants went forward with the real-time experiments, which may not accurately represent the whole. However, with such large differences in decoding accuracies, certain observations can be made from these results. Decoding accuracy drops significantly, as apparent in both multi-session and single-session experiments, where average online accuracies only reach above 90% when 3 classes are being decoded. Additionally, it is important not to take into consideration only the average accuracy achieved by the model when evaluating the model's performance. For example, when 6 classes were decoded in the multi-session experiments, subject 1 achieved an online accuracy of 79.72% (see Table 4). However, on inspecting the recall and precision, when broken down by grasps, the decoding accuracy for grasp 4 and 5 is not high enough for consistent performance. This means that only 3 of the grasps + rest can be used practically, while the other ones would present a high level of misclassification. It is possible that because we are decoding grasps, movements are less discernible, as described in [34], and so if a higher accuracy is desired for a prosthetic control system, developers may choose to sacrifice intuitivity and map more distinct gestures. Of course, 10 class decoding is not necessary for real-time prosthetic control, so we may consider using only 5 classes for robustness, also at the expense of intuitivity and dexterity. Convenience also becomes an issue, with the data collection times for the offline decoding models taking around 40 minutes per subject (including breaks to prevent fatigue). Data collection had to be halved for the real-time experiments, further compromising the accuracy of the machine learning models. We can also note that during the single-session experiments, as the armband is worn for long periods of time, the accuracy of the model decreases more significantly when compared to the multi-session experiments, where the armband is taken off between sessions. This means that ideally, data is frequently recollected, otherwise systems to prevent or mitigate sensor shift and fatigue may be of interest to implement in the future. The subjects wore the armband for a total of 1 hour and 30 minutes. The online decoding accuracies for 10 classes were 34.66% and 18.99% (See Table 6) for subjects 1 and 2 respectively, while with data recollection, the accuracies were 70.96% and 61.77% respectively (Table 4). Retraining models after short usage sessions also becomes impractical, as the experimental time of the multi-session experiments was 1 hour and 10 minutes when only 3, 6, and 10 classes were collected. This accuracy drop could result from user fatigue, sweating, or drifting sensor readings. It is worth mentioning that these factors, such as being prone to fatigue, also affect other MuMIs, such as EMG-based interfaces. Often, offline and real-time results are poorly correlated, making prosthetic control difficult. However, some researchers such as Jiang et al. [50] have suggested that precise mapping from signals to motors may not be necessary and that users will, based on feedback, compensate for poor real-time decoding. Thus, it may be beneficial to design robust feedback systems

TABLE 6. Online decoding accuracies achieved during the single-session experiments. Data was collected a single time and used to train 8 models of differing numbers of classes. This is compared to the accuracy when the same models were tested offline.

Subject	Number of classes decoded	Offline accuracy as tested on the 4th rep	Average online accuracy
1	3	96.90	100
	4	97.13	88.73
	5	96.44	77.10
	6	89.11	62.19
	7	88.6	53.61
	8	85.55	52.29
	9	77.56	38.33
	10	74.1	34.66
2	3	91.22	99.55
	4	90.69	80.63
	5	90.49	58.66
	6	86.04	37.88
	7	80.79	36.94
	8	81.19	20.98
	9	80.00	20.69
	10	74.87	18.99

for the user in conjunction with this so as to have other reliable sources of feedback besides visuals. Shared control systems have also been considered for prosthetic control [51] to reduce user efforts, preventing fatigue and frustration. Shared control frameworks leverage user input and autonomous control to improve task execution, enhance safety, and reduce cognitive and physical effort for the user. Additionally, to reduce the time needed to re-collect data, perhaps transfer and few-shot learning methods [52] may be of interest to employ.

VI. CONCLUSION

In this paper, a new high-density LMG armband is presented employing 40 phototransistors densely fitted around the arm, alongside an armband cover to block out environmental lighting. Compared to the previous armband, the new armband is manufactured on a flexible printed circuit board, offering more reliability and recording data at a higher resolution. The offline and online decoding capabilities of models trained with signals from the HDLMG armband are then explored and compared. Offline experiments were conducted on 10 participants, in which 10 repetitions of 10 classes were collected to train machine learning models. RF and CNN models were trained, with both models reaching accuracies above 91% up to 97.83%. Although CNNs performed slightly better, RFs offer faster training times and are more suited for lower amounts of data. Real-time experiments involving 2 participants were then conducted, testing RF models that decoded 3, 6, and 10 classes.

New data was collected before each model was trained, and the output of the model was used to calculate the online accuracy. There was a large drop in the accuracies compared to the offline results, with 10 class classification models achieving accuracies of 70.96% and 61.77%. However, in some cases with lower numbers of decoded grasps, an increase in online decoding could be seen, indicating that external factors or even small changes in the model's learning can affect the performance of the deployed models.

Therefore, another real-time experiment was conducted, this time with only a single 10 class data collection session. Separate models were then trained for 3 to 10 classes and deployed online. This lead to a more consistent pattern seeing the online accuracy, however, as 10 classes were being decoding, the accuracy was now even lower at 34.66% and 18.99%. Likely, the cause for this low accuracy was the long session time in which the participants had to wear the armband. In this time, conditions gradually change from the time that data was collected, for example, participants will fatigue, sweat, and move their arm's resting position. Sensor readings may also drift. It is apparent that as we move from offline analysis to practical real-time deployment, many issues can arise.

In the future, more robust methods of real-time deployment may be implemented, for example, shared control methods have been employed in EMG systems that can similarly be used for LMG. Issues such as sensor drift that possibly affect real-time accuracy can also be isolated and examined more closely for greater insight. Additionally, with improvements in LMG technology, LMG-based real-time decoding can be benchmarked more comparatively with EMG-based real-time decoding.

ACKNOWLEDGMENT

The authors would like to thank Angus Lynch for his help in soldering FPC components.

REFERENCES

[1] K. Hagberg and R. Brånemark, "Consequences of non-vascular trans-femoral amputation: A survey of quality of life, prosthetic use and problems," *Prosthetics Orthotics Int.*, vol. 25, no. 3, pp. 186–194, 2001.

[2] C. H. Jang, H. S. Yang, H. E. Yang, S. Y. Lee, J. W. Kwon, B. D. Yun, J. Y. Choi, S. N. Kim, and H. W. Jeong, "A survey on activities of daily living and occupations of upper extremity amputees," *Ann. Rehabil. Med.*, vol. 35, no. 6, p. 907, 2011.

[3] I. Dudkiewicz, R. Gabrielov, I. Seiv-Ner, G. Zelig, and M. Heim, "Evaluation of prosthetic usage in upper limb amputees," *Disability Rehabil.*, vol. 26, no. 1, pp. 60–63, Jan. 2004.

[4] K. Østlie, I. M. Lesjø, R. J. Franklin, B. Garfelt, O. H. Skjeldal, and P. Magnus, "Prosthesis use in adult acquired major upper-limb amputees: Patterns of wear, prosthetic skills and the actual use of prostheses in activities of daily life," *Disab. Rehabil., Assistive Technol.*, vol. 7, no. 6, pp. 479–493, Nov. 2012.

[5] D. Datta and V. Ibbotson, "Prosthetic rehabilitation of upper limb amputees: A five year review," *Clin. Rehabil.*, vol. 5, no. 4, pp. 311–316, Nov. 1991.

[6] A. Saradjian, A. R. Thompson, and D. Datta, "The experience of men using an upper limb prosthesis following amputation: Positive coping and minimizing feeling different," *Disability Rehabil.*, vol. 30, no. 11, pp. 871–883, Jan. 2008.

[7] M. Zecca, S. Micera, M. C. Carrozza, and P. Dario, "Control of multifunctional prosthetic hands by processing the electromyographic signal," *Crit. Rev. Biomed. Eng.*, vol. 45, nos. 1–6, pp. 383–410, 2017.

[8] C. Castellini and P. van der Smagt, "Surface EMG in advanced hand prosthetics," *Biol. Cybern.*, vol. 100, no. 1, pp. 35–47, Jan. 2009.

[9] M. B. I. Reaz, M. S. Hussain, and F. Mohd-Yasin, "Techniques of EMG signal analysis: Detection, processing, classification and applications," *Biol. Procedures Online*, vol. 8, no. 1, pp. 11–35, Dec. 2006.

[10] Z. Yang, D. Jiang, Y. Sun, B. Tao, X. Tong, G. Jiang, M. Xu, J. Yun, Y. Liu, B. Chen, and J. Kong, "Dynamic gesture recognition using surface EMG signals based on multi-stream residual network," *Frontiers Bioeng. Biotechnol.*, vol. 9, Oct. 2021, Art. no. 779353.

[11] W. Huo, S. Mohammed, J. C. Moreno, and Y. Amirat, "Lower limb wearable robots for assistance and rehabilitation: A state of the art," *IEEE Syst. J.*, vol. 10, no. 3, pp. 1068–1081, Sep. 2016.

[12] S. Jiang, P. Kang, X. Song, B. P. L. Lo, and P. B. Shull, "Emerging wearable interfaces and algorithms for hand gesture recognition: A survey," *IEEE Rev. Biomed. Eng.*, vol. 15, pp. 85–102, 2022.

[13] J. M. Fajardo, O. Gomez, and F. Prieto, "EMG hand gesture classification using handcrafted and deep features," *Biomed. Signal Process. Control*, vol. 63, Jan. 2021, Art. no. 102210.

[14] S. Fuentes del Toro, Y. Wei, E. Olmeda, L. Ren, W. Guowu, and V. Díaz, "Validation of a low-cost electromyography (EMG) system via a commercial and accurate EMG device: Pilot study," *Sensors*, vol. 19, no. 23, p. 5214, Nov. 2019.

[15] R. Merletti, M. Aventaggiato, A. Botter, A. Holobar, H. Marateb, and T. M. M. Vieira, "Advances in surface EMG: Recent progress in detection and processing techniques," *Crit. Rev. Biomed. Eng.*, vol. 38, no. 4, pp. 305–345, 2010.

[16] W. J. Gaine, C. Smart, and M. Bransby-Zachary, "Upper limb traumatic amputees: Review of prosthetic use," *J. Hand Surgery*, vol. 22, no. 1, pp. 73–76, Feb. 1997.

[17] Y. P. Zheng, M. M. F. Chan, J. Shi, X. Chen, and Q. H. Huang, "Sonomyography: Monitoring morphological changes of forearm muscles in actions with the feasibility for the control of powered prosthesis," *Med. Eng. Phys.*, vol. 28, no. 5, pp. 405–415, Jun. 2006.

[18] A. S. Dhawan, B. Mukherjee, S. Patwardhan, N. Akhlaghi, G. Diao, G. Levay, R. Holley, W. M. Joiner, M. Harris-Love, and S. Sikdar, "Proprioceptive sonomyographic control: A novel method for intuitive and proportional control of multiple degrees-of-freedom for individuals with upper extremity limb loss," *Sci. Rep.*, vol. 9, no. 1, p. 9499, Jul. 2019.

[19] X. Chen, Y.-P. Zheng, J.-Y. Guo, and J. Shi, "Sonomyography (SMG) control for powered prosthetic hand: A study with normal subjects," *Ultrasound Med. Biol.*, vol. 36, no. 7, pp. 1076–1088, Jul. 2010.

[20] X. Jiang, L.-K. Merhi, Z. G. Xiao, and C. Menon, "Exploration of force myography and surface electromyography in hand gesture classification," *Med. Eng. Phys.*, vol. 41, pp. 63–73, Mar. 2017.

[21] Z. G. Xiao and C. Menon, "A review of force myography research and development," *Sensors*, vol. 19, no. 20, p. 4557, Oct. 2019.

[22] M. U. Rehman, K. Shah, I. U. Haq, S. Iqbal, and M. A. Ismail, "A wearable force myography-based armband for recognition of upper limb gestures," *Sensors*, vol. 23, no. 23, p. 9357, Nov. 2023.

[23] S. Wilson and R. Vaidyanathan, "Upper-limb prosthetic control using wearable multichannel mechanomyography," in *Proc. Int. Conf. Rehabil. Robot. (ICORR)*, Jul. 2017, pp. 1293–1298.

[24] J. Silva, W. Heim, and T. Chau, "A self-contained, mechanomyography-driven externally powered prosthesis," *Arch. Phys. Med. Rehabil.*, vol. 86, no. 10, pp. 2066–2070, Oct. 2005.

[25] E. Cho, R. Chen, L.-K. Merhi, Z. Xiao, B. Pousett, and C. Menon, "Force myography to control robotic upper extremity prostheses: A feasibility study," *Frontiers Bioeng. Biotechnol.*, vol. 4, p. 18, Mar. 2016.

[26] M. Shahmohammadi, B. Guan, R. V. Godoy, A. Dwivedi, P. Nielsen, and M. Liarokapis, "On lightmyography based muscle-machine interfaces for the efficient decoding of human gestures and forces," *Sci. Rep.*, vol. 13, no. 1, p. 327, Jan. 2023.

[27] M. Shahmohammadi, A. Dwivedi, P. Nielsen, A. Taberner, and M. Liarokapis, "On lightmyography: A new muscle machine interfacing method for decoding human intention and motion," in *Proc. 43rd Annu. Int. Conf. IEEE Eng. Med. Biol. Soc. (EMBC)*, Nov. 2021, pp. 4744–4748.

[28] L. Finlayson, I. R. M. Barnard, L. Mcmillan, S. H. Ibbotson, C. T. A. Brown, E. Eadie, and K. Wood, "Depth penetration of light into skin as a function of wavelength from 200 to 1000 nm," *Photochem. Photobiol.*, vol. 98, no. 4, pp. 974–981, Jul. 2022.

[29] J. Allen, "Photoplethysmography and its application in clinical physiological measurement," *Physiological Meas.*, vol. 28, no. 3, pp. R1–R39, Mar. 2007.

[30] M. Atzori, A. Gijsberts, C. Castellini, B. Caputo, A.-G.-M. Hager, S. Elsig, G. Giatsidis, F. Bassetto, and H. Müller, "Electromyography data for non-invasive naturally-controlled robotic hand prostheses," *Sci. Data*, vol. 1, no. 1, pp. 1–13, Dec. 2014.

[31] J.-U. Chu, I. Moon, and M.-S. Mun, "A real-time EMG pattern recognition system based on linear-nonlinear feature projection for a multifunction myoelectric hand," *IEEE Trans. Biomed. Eng.*, vol. 53, no. 11, pp. 2232–2239, Nov. 2006.

[32] Z. O. Khokhar, Z. G. Xiao, and C. Menon, "Surface EMG pattern recognition for real-time control of a wrist exoskeleton," *Biomed. Eng. OnLine*, vol. 9, no. 1, pp. 1–17, Dec. 2010.

[33] Z. G. Xiao and C. Menon, "Towards the development of a wearable feedback system for monitoring the activities of the upper-extremities," *J. NeuroEng. Rehabil.*, vol. 11, no. 1, p. 2, 2014.

[34] M. Zanghieri, S. Benatti, A. Burrello, V. Kartsch, F. Conti, and L. Benini, "Robust real-time embedded EMG recognition framework using temporal convolutional networks on a multicore IoT processor," *IEEE Trans. Biomed. Circuits Syst.*, vol. 14, no. 2, pp. 244–256, Apr. 2020.

[35] H. Daley, K. Englehart, L. Hargrove, and U. Kuruganti, "High density electromyography data of normally limbed and transradial amputee subjects for multifunction prosthetic control," *J. Electromyogr. Kinesiol.*, vol. 22, no. 3, pp. 478–484, Jun. 2012.

[36] A. Stango, F. Negro, and D. Farina, "Spatial correlation of high density EMG signals provides features robust to electrode number and shift in pattern recognition for myocontrol," *IEEE Trans. Neural Syst. Rehabil. Eng.*, vol. 23, no. 2, pp. 189–198, Mar. 2015.

[37] D. Staudenmann, I. Kingma, D. F. Stegeman, and J. H. van Dieën, "Towards optimal multi-channel EMG electrode configurations in muscle force estimation: A high density EMG study," *J. Electromyogr. Kinesiol.*, vol. 15, no. 1, pp. 1–11, Feb. 2005.

[38] S. Tam, G. Bilodeau, J. Brown, G. Gagnon-Turcotte, A. Campeau-Lecours, and B. Gosselin, "A wearable wireless armband sensor for high-density surface electromyography recording," in *Proc. 41st Annu. Int. Conf. IEEE Eng. Med. Biol. Soc. (EMBC)*, Jul. 2019, pp. 6040–6044.

[39] T. Feix, J. Romero, H.-B. Schmiedmayer, A. M. Dollar, and D. Kragic, "The GRASP taxonomy of human grasp types," *IEEE Trans. Hum.-Mach. Syst.*, vol. 46, no. 1, pp. 66–77, Feb. 2016.

[40] S. Ioffe and C. Szegedy, "Batch normalization: Accelerating deep network training by reducing internal covariate shift," in *Proc. Int. Conf. Mach. Learn.*, Jan. 2015, pp. 448–456.

[41] M. Asghari Oskoei and H. Hu, "Myoelectric control systems—A survey," *Biomed. Signal Process. Control*, vol. 2, no. 4, pp. 275–294, Oct. 2007.

[42] K. Englehart, B. Hudgin, and P. A. Parker, "A wavelet-based continuous classification scheme for multifunction myoelectric control," *IEEE Trans. Biomed. Eng.*, vol. 48, no. 3, pp. 302–311, Mar. 2001.

[43] T. K. Ho, "Random decision forests," in *Proc. 3rd Int. Conf. Document Anal. Recognit.*, vol. 1, Aug. 1995, pp. 278–282.

[44] S. Y. Ali and H. Maseeh, "Dropout: An effective approach to prevent neural networks from overfitting," *Asian J. Res. Comput. Sci.*, vol. 18, no. 2, pp. 163–185, Feb. 2025.

[45] D. P. Kingma and J. Ba, "Adam: A method for stochastic optimization," in *3rd Int. Conf. Learn. Represent., (ICLR)*, Dec. 2014, pp. 1–15.

[46] J. Chapman, A. Dwivedi, and M. Liarokapis, "A wearable, open-source, lightweight forcemyography armband: On intuitive, robust muscle-machine interfaces," in *Proc. IEEE/RSJ Int. Conf. Intell. Robots Syst. (IROS)*, Sep. 2021, pp. 4138–4143.

[47] R. V. Godoy, B. Guan, A. Dwivedi, and M. Liarokapis, "An affordances and electromyography based telemanipulation framework for control of robotic arm-hand systems," in *Proc. IEEE/RSJ Int. Conf. Intell. Robots Syst. (IROS)*, Oct. 2023, pp. 6998–7004.

[48] R. V. Godoy, A. Dwivedi, B. Guan, A. Turner, D. Shieff, and M. Liarokapis, "On EMG based dexterous robotic telemanipulation: Assessing machine learning techniques, feature extraction methods, and shared control schemes," *IEEE Access*, vol. 10, pp. 99661–99674, 2022.

[49] R. V. Godoy, B. Guan, A. Dwivedi, M. Shahmohammadi, M. Owen, and M. Liarokapis, "Multi-grasp classification for the control of robot hands employing transformers and lightmyography signals," in *Proc. 45th Annu. Int. Conf. IEEE Eng. Med. Biol. Soc. (EMBC)*, Jul. 2023, pp. 1–6.

[50] N. Jiang, I. Vujaklija, H. Rehbaum, B. Graimann, and D. Farina, "Is accurate mapping of EMG signals on kinematics needed for precise online myoelectric control?" *IEEE Trans. Neural Syst. Rehabil. Eng.*, vol. 22, no. 3, pp. 549–558, May 2014.

[51] C. Cipriani, F. Zaccone, S. Micera, and M. Chiara Carrozza, "On the shared control of an EMG-controlled prosthetic hand: Analysis of user–prosthesis interaction," *IEEE Trans. Robot.*, vol. 24, no. 1, pp. 170–184, Feb. 2008.

[52] R. V. Godoy, B. Guan, F. Sanches, A. Dwivedi, and M. Liarokapis, "Electromyography based gesture decoding employing few-shot learning, transfer learning, and training from scratch," *IEEE Access*, vol. 11, pp. 104142–104154, 2023.

BONNIE GUAN (Student Member, IEEE) received the Bachelor of Engineering degree (Hons.) in mechatronics engineering from The University of Auckland, New Zealand, in 2022, where she is currently pursuing the Ph.D. degree with the New Dexterity Research Group. Her work focuses on exploring novel methods for developing human–machine interfaces to facilitate an intuitive and dexterous control of robotic and prosthetic devices.

RICARDO V. GODOY (Student Member, IEEE) received the Bachelor of Engineering degree in mechatronics engineering and the M.Sc. degree in mechanical engineering from the University of São Paulo, São Carlos, Brazil, in 2019 and 2021, respectively. He is currently pursuing the Ph.D. degree in mechatronics engineering with the New Dexterity Research Group, The University of Auckland, New Zealand. He works on the analysis and development of novel human–machine interfaces (HMI) for the control of robotic and bionic devices while focusing on the challenges and limitations in the use of HMI for robust grasping and decoding of dexterous, in-hand manipulation tasks. He also works on the development of novel and robust deep learning-based solutions for bio-signals analyses and processing.

MOJTABA SHAHMOHAMMADI received the master's degree in mechanical engineering from Sharif University and the Ph.D. degree in mechanical engineering from The University of Auckland. He also was a Professional Staff Member in designing robotic grippers and a Graduate Teaching Assistant with The University of Auckland. He is currently a Product Development Engineer with the Fisher and Paykel Healthcare, New Zealand. His expertise spans CAD/CAM, Abaqus, and sensor technologies. Previously, he was a Quality Assurance Manager with Electro BC, Tehran, Iran. His research focused on developing prosthetic hands using rapid prototyping techniques and designing human–machine interfaces to enhance communication between humans and robotic devices.

ANANY DWIVEDI received the B.Tech. degree in electronics and communication engineering from the LNM Institute of Information Technology, Jaipur, India, in 2015, the M.S. degree in robotics engineering from Worcester Polytechnic Institute (WPI), Worcester, MA, USA, in 2017, and the Ph.D. degree from the New Dexterity Research Group, The University of Auckland, New Zealand. Currently, he is a Postdoctoral Researcher with the Artificial Intelligence Institute, University of Waikato, New Zealand, focusing on the applications of machine learning techniques in data stream adaptation and interpretation for weak signals and extreme events. His work focused on deciphering the myoelectric activity of the muscles of the human forearm and hand to decode dexterous manipulation motions in real and virtual environments. He joined the Chair of the Autonomous Systems and Mechatronics, Friedrich-Alexander-Universität-Erlangen-Nürnberg, Germany, as a Postdoctoral Researcher after his Ph.D. His work focused on the development of bi-directional human–machine interfaces to increase presence and embodiment of the user during interaction with virtual environments while considering human-centered design principles.

MINAS LIAROKAPIS (Senior Member, IEEE) received the Diploma degree in computer engineering from the University of Patras, Patras, Greece, the M.Sc. degree in information technologies in medicine and biology from the National and Kapodistrian University of Athens, Athens, Greece, and the Ph.D. degree in mechanical engineering from the National Technical University of Athens, Athens. He is currently an Associate Professor with the Department of Mechanical and Mechatronics Engineering, The University of Auckland, New Zealand, the Director of the New Dexterity Research Group (www.newdexterity.org), and the Chair of New Zealand Robotics, Automation, and Sensing (www.nzras.org.nz). He is the Founder of the OpenBionics Initiative (www.openbionics.org) and the Co-Founder of OpenRobotHardware (www.openrobothardware.org) and HandCorpus (www.handcorpus.org). His research interests include providing robotics solutions to everyday life problems, modeling, designing, and controlling novel robotics and bionics hardware.